

R-C-P Method: An Autonomous Volume Calculation Method Using Image Processing and Machine Vision

MA Muktadir , Sydney Parker, and Sun Yi

Abstract: Machine vision and image processing are often used with sensors for situation awareness in autonomous systems, from industrial robots to self-driving cars. The 3D depth sensors, such as LiDAR (Light Detection and Ranging), Radar, are great invention for autonomous systems. Due to the complexity of the setup, LiDAR may not be suitable for some operational environments, for example, a space environment. This study was motivated by a desire to get real-time volumetric and change information with multiple 2D cameras instead of a depth camera. Two cameras were used to measure the dimensions of a rectangular object in real-time. The R-C-P (row-column-pixel) method is developed using image processing and edge detection. In addition to the surface areas, the R-C-P method also detects discontinuous edges or volumes. Lastly, experimental work is presented for illustration of the R-C-P method, which provides the equations for calculating surface area dimensions. Using the equations with given distance information between the object and the camera, the vision system provides the dimensions of actual objects.

Keywords: Image processing; Edge Detection; Machine Vision; Volume Calculation; R-C-P method

1. Introduction

Many touchless maintenance systems require volumetric information, for example, in object monitoring and defect detecting. As an example of quantifying concrete spalling damage using depth cameras or 3D scanners, a faster R-CNN-based concrete spalling damage detection method was developed [1]. Using a single aerial image, a study proposes a deep learning-based approach for detecting and reconstructing buildings. An optimized multi-scale convolutional-deconvolutional network is used to obtain the required knowledge to reconstruct the 3D shapes of buildings, including height data and linear elements of individual roofs [2].

A novel solution to the problem of depth reconstruction from a single image was presented by Hassner et al.. 3D reconstruction from a single view is an ill-posed problem. A synthesis approach based on examples is used by the authors to address this problem. Their method involves using a database containing examples of mappings from appearance to depth for objects in a single class (e.g., hands, human figures). An image of a novel object is combined with the known depths of patches from similar objects to produce a plausible depth estimate [3].

Patterned textures are good for conveying 3D images due to two key ingredients: texel distortion and texel distortion rate variation within the texture region. This is also known as a texture gradient. The output of shape-from-texture algorithms is generally a dense map of surface normal. With a smooth textured surface, this is feasible for recovering 3D shapes [4], [5].

The use of machine learning, machine vision, and image processing have been used to identify manufacturing defects and avoid obstructions in robotics. RGB and depth cameras are not only used for taking pictures but also as nondestructive sensors [6-9]. 2D to 3D conversion algorithms based on image processing can be split into two groups according to the number of input images: algorithms using more than one image and algorithms using one image. For algorithms based on two or more images, typically, more than one input image is taken from a single camera with moving objects in the scene, or by multiple fixed cameras at different viewing angles. First-group depth cues are called binocular or multi-ocular depth cues. In the second group of depth cues, monocular depth cues are based on a single still image [10].

Binocular disparity, Motion, Defocus, Focus, and Silhouette are the depth cues of binocular or multi-ocular. The binocular disparity can be utilized to determine an object's depth by comparing two images from slightly different viewpoints of the same scene. Objects closer to the viewing camera move across the retina more rapidly than objects farther away, which provides an important cue to depth perception. Based on the degree of blurring present in an

image, depth-from-defocus methods generate a depth map. There is a close relation between the depth-from-focus algorithm and the depth-from-defocus algorithm. By varying and registering the distance between the camera and the scene, depth-from-focus requires a series of images of the scene with various focus levels, while using depth-from-defocus, two or more images are required with fixed camera and object positions with different focal settings. Silhouettes in images refer to the contours separating objects from their backgrounds. It is necessary to take multiple views of the scene from different points of view to use shape-from-silhouette methods [10]-[12].

Defocus, Linear perspective, Atmosphere Scattering, Shading, Patterned texture, Symmetric patterns, Occlusion, Statistical patterns are the depth cues of monocular. The algorithms in this group are based on depth-from-defocus from a single image, which requires images taken using different focal settings. According to linear perspective, parallel lines, such as rail tracks, appear to merge with distance, eventually vanishing at the horizon. In general, the more converged the lines, the further they seem to be [8]. Through a diffusion of radiation in the atmosphere, light propagation through the atmosphere is affected in the sense that its direction and power are altered. It is this effect that creates the phenomenon known as atmosphere scattering, otherwise known as haze, resulting in various visual effects, such as distant objects appearing bluish, and flashlight beams becoming diffused. Object shapes are encoded in the image by the gradual variation of surface shading. Two key factors contribute to a good 3D impression with patterned textures: texel distortions and changes in texel distortion across texture regions. Natural or man-made scenes often feature symmetrical patterns. By using symmetric patterns, 3D reconstruction is possible based on two images of a bilaterally symmetric object from different angles. Objects that overlap or partially obscure another object are considered closer according to depth-from-occlusion algorithms. A statistical pattern is a pattern that occurs repeatedly in images. Machine learning techniques can be effective when input data is large in number or dimension [10], [13], [14].

According to the literature review, depth information has been considered mostly when constructing 3D or extracting information from 2D images. This study developed a new R-C-P method based on the image unit. Python is used to retrieve real-time 3D data from 2D cameras.

2. Materials and Methods

The primary data used in image processing applications is images. Various types of images are used in data analysis, including RGB, grayscale, and binary images. As a digital image is a two-dimensional array of data, a pixel is the smallest unit of the image that can be controlled and addressed by coordinates, and its intensity varies [15]. After capturing RGB images, the Python algorithm converted them to grayscale images and after detecting edges, binary images were used to develop the R-C-P algorithm.

2.1. Proposed method

A flow chart of the proposed method is shown in Figure 1.

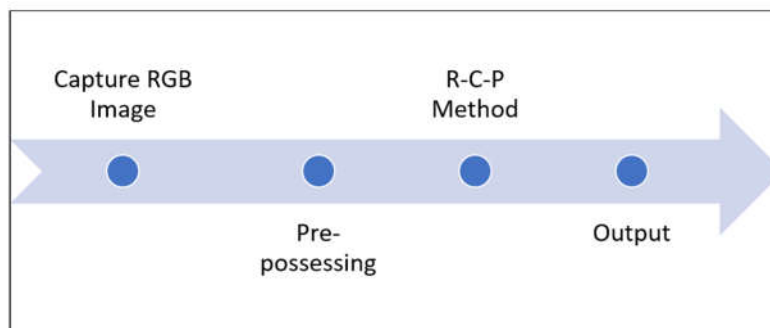


Figure 1. Method flow chart.

2.1.1. Capturing RGB images.

For taking pictures of two surfaces of a rectangular object, two cameras have been considered and set up. Figure 2 illustrates an experimental setup using two Intel RealSense cameras.



Figure 2. Experimental setup.

2.1.2. Pre-processing.

The pre-processing sections are divided into two parts: conversion of RGB images into grayscale images and edge detection of grayscale images.

1. RGB to GRAY scale

An RGB image consists of three colors. Each RGB color represents one of the three basic color components Red, Green, and Blue. This RGB color image has 24 bits per pixel - 8 bits per color band (red, green, blue). The smallest unit of each color is the pixel, which has 256 values (0-255). The color of an image can be modified by varying the number of each unit of each color band. Grayscale images, on the other hand, are represented by intensity values. There are many shades of gray between black and white in grayscale images. Each pixel's intensity is based on a range between zero and one (minimum and maximum) and on varying shades of gray that range between 0 and 255 [15].

RGB images contain three color channels, with each small square box representing one pixel.

For example, if we consider a pixel of each channel in a specific location (n, m) and set a value of 0 for the red channel, 255 for the green channel, and 0 for the blue channel, the output image will be a solid green image as the intensity of the green channel is the maximum. As part of this study, the RGB images captured by the camera were first converted to grayscale images, Figure 4.

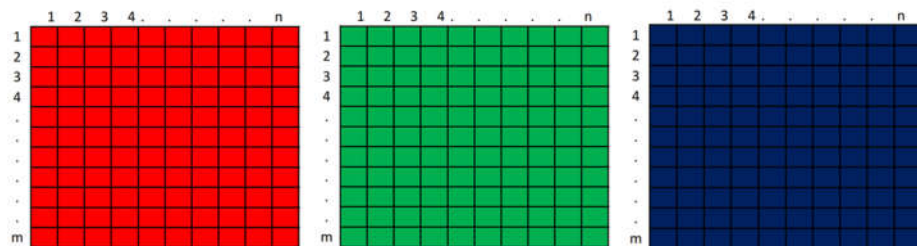


Figure 3. Left to right, RGB pixels are represented as Red, Green, and Blue.

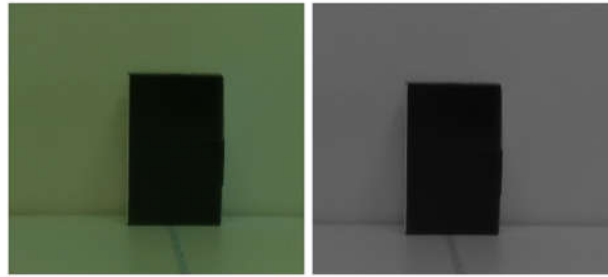


Figure 4. The RGB image (left) and the grayscale image (right).

2. Canny Edge Detection

The edges of images refer to pixels whose gray levels change suddenly, which is the most basic feature of an image. Based on gray discontinuous points, edge detection is a basic method for recognizing and segmenting images. John F. Canny proposed the Canny operator in 1986 as a multiply-scale algorithm for edge detection. It is widely used in the field of image processing [16].

The steps for Canny edge detection are usually divided into several sections:

1. Usually, the Gauss smoothing filter is used to reduce noise in the image before detecting the edge.
2. Calculate the gradient magnitude and orientation using finite-difference approximations for the partial derivatives. The gradient direction usually corresponds to the four angles - 0, 45, 90, and 135 degrees.
3. Non-maximum suppression, thus removing non-edge pixels, leaving only fine lines.
4. Set the hysteresis threshold; a hysteresis threshold requires two thresholds that are either retained or excluded to select the edge.

When the magnitude of a pixel position exceeds a high threshold, it is reserved as an edge pixel. An excluded pixel is one whose magnitude is below the high threshold. Pixel positions between the two thresholds are reserved only when connected to pixels higher than the high threshold [17]-[19].

2.1.3. R-C-P Method

Detection of edges is displayed as a binary image, which is the simplest type of image and has two values, '0' and '1' or 255. Since each pixel is represented by one binary digit, a binary image is called a 1-bit/pixel image. This R-C-P method uses this black-and-white unit pixel. Figure 5 shows an example of a binary image after edge detection, where white pixels (1 or 255) indicate the edges of the images. Initially, the R-C-P method considers each white pixel in row directions.

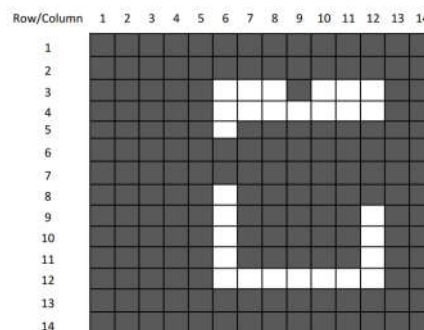


Figure 5. R-C-P method, step 1.

A second step involves searching for any other white pixel in its parallel (row) direction and turning a black pixel (0) into a white pixel between these two parallel white pixels.

As can be seen from Figures 5 and 6, there is no parallel white pixel in the row direction of (5,6), so there is no change in black pixels in its row direction. On the other hand, if we look at the row and column location of (9,6), it converts all the black pixels between (9,6) and (9,12).

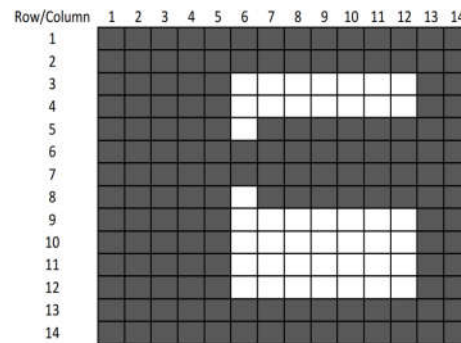


Figure 6. R-C-P step 2.

In the third step, the R-C-P method algorithm considers each white pixel in column directions and searches for any other white pixel in its parallel (column) direction, and if it detects, then the algorithm converts the black pixel (0) into a white pixel between these two parallel pixels. Figure 7 shows how the black in the position of (6,6) and (7,6) is converted to white by the location of (5,6) and (8,6) being parallel in the vertical direction.

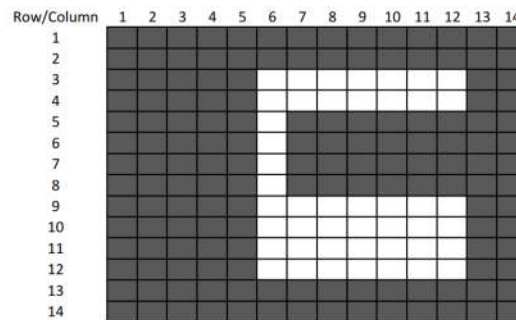


Figure 7. R-C-P method step 3.

In Figure 8, the conversion from 0 to 255 has been completed after the search in column direction has been completed.

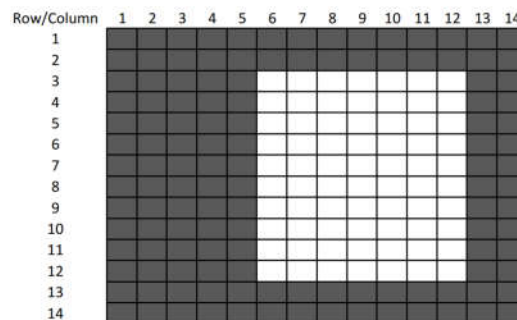


Figure 8. R-C-P method output.

It is easy to calculate the area of a surface by calculating the total number of white pixels in the output since 1 pixel corresponds to 0.264 mm. In this study, the goal is to obtain the volume of a rectangular object from a camera in real-time. Unless we get at least a length of width or height of the output white pixel area, the surface alone will not provide us with the volume, even though we set four cameras in all directions. Thus, the width and height calculations are added in the R-C-P method in the final steps.

Two cameras are considered in this study. Assume camera 1 has 'l' number of white pixels, 'p' is the number of rows left in the output (255) areas, and 'q' is the number of columns left in the output (255) areas. In camera 2, let's say there are 'w' white pixels, 'x' is the number of rows in the output (255) areas, and 'y' is the number of columns in the output (255) areas.

The detected surface areas have the following width, height, and volume, as shown in Equation 1.

For camera 1,

Width/row, $W1 = (l/p) * 0.264 \text{ mm}$

Height/column, $H1 = (l/q) * 0.264 \text{ mm}$

For camera 2,

Width/row, $W2 = (w/x) * 0.264 \text{ mm}$

Height/column, $H2 = (w/y) * 0.264 \text{ mm}$

The volume of the rectangular object,

$$V = W1 * \{(H1+H2)/2\} * W2 \text{ mm}^3 \quad (1)$$

In Equation 1, the volume is given in real-time. As a 2D camera uses as a sensor, this volume may not be the same as the actual dimensions of the object. The experiment presented in the following section uses the R-C-P method to get the relationship between the actual and predicted surfaces.

3. Experimental Results

To validate the R-C method and to reduce the error between the predicted and actual dimensions of the object, an experimental study was conducted, and three sizes of rectangular objects were considered. The experimental setup and dimensions of three rectangular surfaces are shown in Figure 9. The objective of this experiment was to calculate and analyze the surface area of the object by varying the distance from the object's surface and the camera distance.

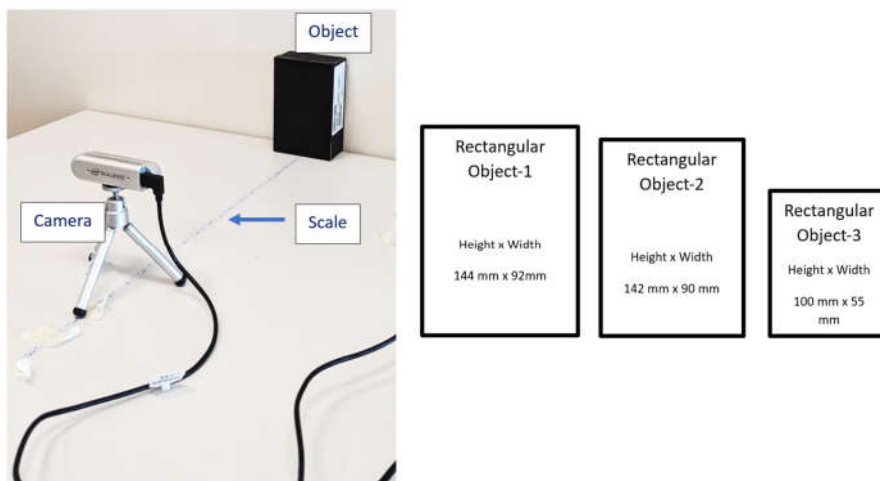


Figure 9. Setup and dimensions of the experimental objects.

Distance x (object surface to camera) varies between 200 mm and 700 mm. However, after running the R-C method, the algorithm result started when $x=395$ mm. Figure 10 shows the output of RGB, Edge, and R-C-P methods.

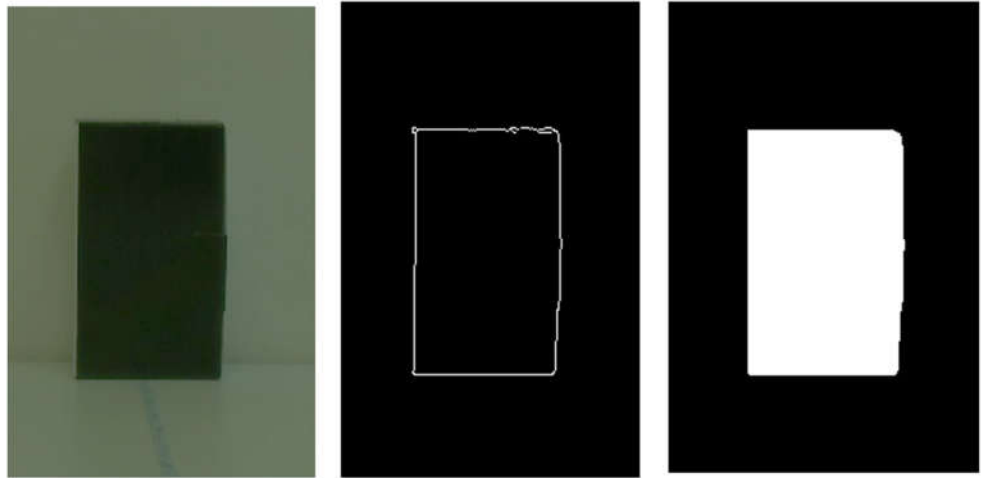


Figure 10. The RGB, Edge, and R-C-P methods detected surfaces (left to right).

Figure 11 illustrates that the R-C-P algorithm can detect the surface area as white pixels without detecting the complete edges.

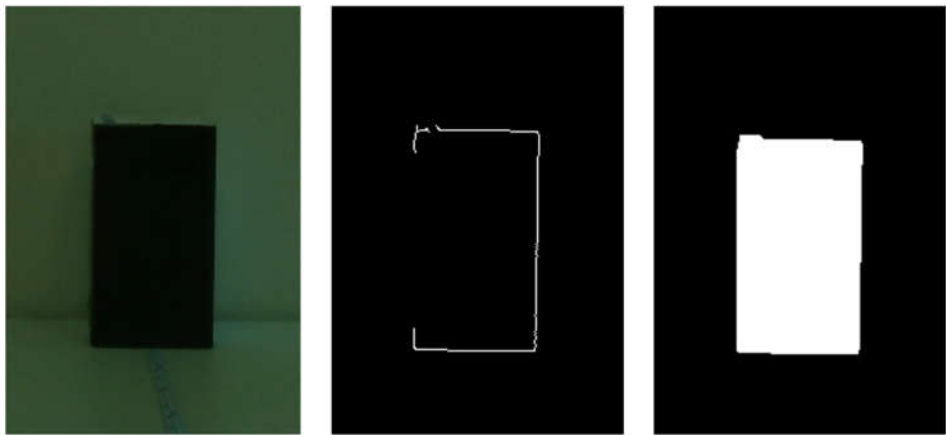


Figure 11. R-C-P method output (right), incomplete edge detection (middle), and RGB image (left).

After completing several experiments, actual and R-C-P methods were used to calculate the width (row) and height (column). The data in Table 1 shows the width of objects-1,2, and 3, where x is the distance between the object's face and camera location.

Table 1. A comparison of the actual and R-C-P widths of the target image surfaces with respect to distances x , where columns D, G, and J indicate the ratio between the actual and R-C-P measurements.

A	OBJECT-1			OBJECT-2			OBJECT-3		
	B	C	D	E	F	G	H	I	J
x (mm)	width/row (mm)	R-C-P Method (mm)	D= B/C	width/row (mm)	R-C-P Method (mm)	G=E/F	width/row (mm)	R-C-P Method (mm)	J=H/I
395	55.00	6.87	8.00	90.00	15.85	5.68	92.00	17.16	5.36
445	55.00	5.41	10.17	90.00	12.60	7.14	92.00	13.60	6.76
495	55.00	4.28	12.86	90.00	10.42	8.64	92.00	10.89	8.44
545	55.00	3.62	15.20	90.00	8.51	10.58	92.00	9.01	10.22
595	55.00	3.01	18.26	90.00	7.25	12.41	92.00	7.70	11.95
645	55.00	2.55	21.58	90.00	5.93	15.18	92.00	6.43	14.30

Table 2. A comparison of the actual and R-C-P heights of the target image surfaces with respect to distances x , where columns N, Q, and T indicate the ratio between the actual and R-C-P measurements.

K	OBJECT-1			OBJECT-2			OBJECT-3		
	L	M	N	O	P	Q	R	S	T
x (mm)	height/col- umn (mm)	R-C-P Method (mm)	N=L/M	height/col- umn (mm)	R-C-P Method (mm)	Q=O/P	height/col- umn (mm)	R-C-P Method (mm)	T=R/S
395	100	5.15	19.40	142.00	11.89	11.95	144.00	12.87	11.19
445	100	4.06	24.65	142.00	9.45	15.03	144.00	10.20	14.12
495	100	3.21	31.18	142.00	7.81	18.17	144.00	8.17	17.62
545	100	2.71	36.84	142.00	6.38	22.26	144.00	6.75	21.32
595	100	2.26	44.28	142.00	5.44	26.10	144.00	5.78	24.94
645	100	1.91	52.31	142.00	4.45	31.94	144.00	4.82	29.85

As shown in Figures 12 and 13, there is a graph between the distance and the ratio of the actual object (height/width) dimensions and the R-C-P method. In both graphs, the ratio increases as the distance x increases.

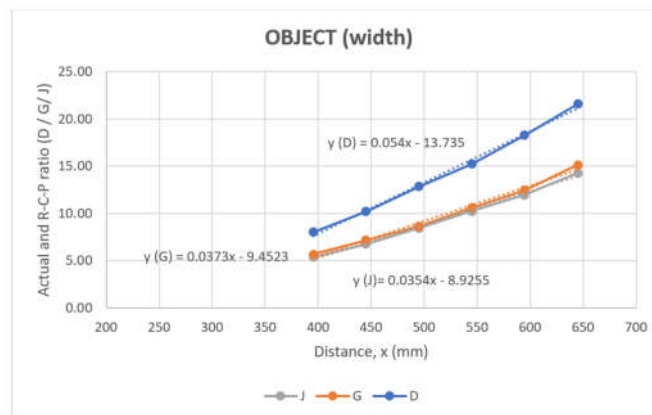


Figure 12. Distance versus ratio (D/G/J).

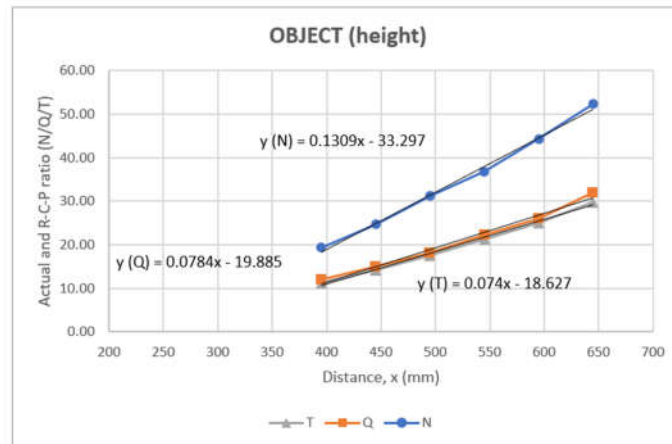


Figure 13. Distance versus ratio (T/Q/N).

Based on the data from Table 1 and Graph 12, equations 2,3 and 4 can be derived. Equation 4 shows that $r1$ represents the ratio of width to row direction, and x represents distance. Moreover, b represents the width of the detected surface from the R-C-P method.

The equation for getting slope:

$$m1 = -0.0064x + 2.4076 \quad (2)$$

The equation for getting intercept:

$$b1 = 0.0661x - 16.807 \quad (3)$$

The ratio of the Actual to R-C-P method in the width direction.

$$r1 = m1 * b + b1 \quad (4)$$

Based on the data from Table 2 and Graph 13, equations 5, 6, and 7 can be derived. Equation 7 shows that $r2$ represents the ratio of width to row direction, and x represents distance. Moreover, h represents the height of the detected surface from the R-C-P method.

The equation for getting slope:

$$m2 = -0.0265x + 9.9751 \quad (5)$$

The equation for getting intercept:

$$b2 = 0.1681x - 42.735 \quad (6)$$

The ratio of the Actual to R-C-P method in the height direction.

$$r2 = m2 * h + b2 \quad (7)$$

Table 3 compares the ratio between actual and R-C-P method data and the ratio derived from equations 4 and 7.

Table 3. A comparison of the ratios in Tables 1 and 2 with the ratios derived from equations 4 and 7.

Surface Width/Row			Surface Height/Column		
R-C-P ratio (From table 1)	Ratio (Equation 4)	Error (%)	R-C-P ratio (From table 2)	Ratio (Equation 7)	Error (%)
8.48	8.00	5.90	21.13	19.40	8.89
7.39	5.68	30.21	17.81	11.95	49.09
7.24	5.36	34.95	17.33	11.19	54.83
10.23	10.17	0.55	24.70	24.65	0.18
7.06	7.14	1.19	14.90	15.03	0.87
6.62	6.76	2.17	13.53	14.12	4.15
12.66	12.86	1.55	30.39	31.18	2.51
7.99	8.64	7.50	15.92	18.17	12.40
7.63	8.44	9.67	14.80	17.62	16.03
15.31	15.20	-0.73	36.75	36.84	0.23
10.03	10.58	5.23	20.38	22.26	8.44
9.49	10.22	7.13	18.70	21.32	12.27
18.31	18.26	0.22	44.20	44.28	0.17
12.36	12.41	0.35	25.77	26.10	1.26
11.74	11.95	1.75	23.83	24.94	4.42
21.44	21.58	0.63	52.08	52.31	0.44
15.63	15.18	2.94	34.05	31.94	6.60
14.76	14.30	3.20	31.36	29.85	5.04

Excluding the distance of 395 mm, the experimental study shows an error of up to 10 percent for the width or row, and usually below 4 percent.

If we exclude the distance $x = 395$ mm, the experimental study shows errors for the height or column length of the detected surface of up to 17 percent, and mostly the errors remain below 7 percent.

3.1. Calculation of the volume from the camera

Based on two cameras, let us assume the width of the surface using the R-C-P method is x_1 and x_2 for camera 1 and camera 2. The height or column for cameras 1 and 2 from the R-C-P method is y_1 and y_2 , respectively.

We can get m_1 , m_2 , b_1 , and b_2 from equations 2,3,5 and 6 if we know the distance of x , from equations 4 and 7.

$$\text{Camera 1: } r_{11} = m_1 * x_1 + b_1$$

$$r_{21} = m_2 * y_1 + b_2$$

$$\text{Camera 2: } r_{12} = m_1 * x_2 + b_1$$

$$r_{22} = m_2 * y_2 + b_2$$

Object width:

$$\text{Camera 1: } w1 = r11 * x1$$

$$\text{Camera 2: } w2 = r12 * x2$$

Object height:

$$\text{Camera 1: } h1 = r21 * y1$$

$$\text{Camera 2: } h2 = r22 * y2$$

$$\text{Volume of the object} = w1 * (h1+h2)/2 * w2$$

4. Discussion

This study introduces a volume calculation method, R-C-P (Row-Column-Pixel), to calculate the volume of a rectangular object without a LiDAR or 3D depth camera. With this method, the data are analyzed to get equations to calculate the detected surface width and column length. Using that equation, the volume of an object can be calculated if the distance between the surface and the camera is known.

It can be used to change the volume change for a specific system in real-time as well as for actual dimensions. The following factors will be considered in future studies to reduce errors in the actual data and the theoretical calculations.

1. The experiment will consider different types of objects.
2. It will be done with different 2D cameras since this experiment has so far only been done with one model. Additionally, four (4) cameras will be used to modify the present algorithm.
3. We will change the experiment setup by adjusting the distance between the camera and the object.

References

- [1] G. H. Beckman, D. Polyzois and Y. Cha, "Deep learning-based automatic volumetric damage quantification using depth camera," *Autom. Constr.*, vol. 99, pp. 114-124, 2019.
- [2] F. Alidoost, H. Arefi and F. Tombari, "2D image-to-3D model: Knowledge-based 3D building reconstruction (3DBR) using single aerial images and convolutional neural networks (CNNs)," *Remote Sensing*, vol. 11, (19), pp. 2219, 2019.
- [3] T. Hassner and R. Basri, "Example based 3D reconstruction from single 2D images," in *2006 Conference on Computer Vision and Pattern Recognition Workshop (CVPRW'06)*, 2006, .
- [4] Q. Wei, "Converting 2d to 3d: A survey," in *International Conference, Page (s)*, 2005, .
- [5] K. Wong and F. Ernst, "No title," *Single Image Depth-from-Defocus*, 2004.
- [6] S. Garfo, M. A. Mukhtadir and S. Yi, "Defect Detection on 3D Print Products and in Concrete Structures Using Image Processing and Convolution Neural Network," 2020.
- [7] M. A. Mukhtadir and S. Yi, "Machine vision-based detection of surface defects of 3D-printed objects," in *2021 ASEE Virtual Annual Conference Content Access*, 2021, .
- [8] S. C. Dekkata *et al*, "LiDAR-Based Obstacle Detection and Avoidance for Navigation and Control of an Unmanned Ground Robot Using Model Predictive Control," 2023.
- [9] S. C. Dekkata *et al*, "No title," *Improved Model Predictive Control System Design and Implementation for Unmanned Ground Vehicles*, 2022.
- [10] Q. Wei, "Converting 2d to 3d: A survey," in *International Conference, Page (s)*, 2005, .
- [11] E. Trucco and A. Verri, *Introductory Techniques for 3-D Computer Vision*. 1998201.
- [12] S. K. Nayar and Y. Nakagawa, "Shape from focus," *IEEE Trans. Pattern Anal. Mach. Intell.*, vol. 16, (8), pp. 824-831, 1994.

- [13] A. R. François, G. G. Medioni and R. Waupotitsch, "Reconstructing mirror symmetric scenes from a single view using 2-view stereo geometry," in *2002 International Conference on Pattern Recognition*, 2002, .
- [14] K. Wong and F. Ernst, "Master thesis "Single Image Depth-from-Defocus," *Delft University of Technology & Philips Natlab Research, Eindhoven, the Netherlands*, 2004.
- [15] K. Padmavathi and K. Thangadurai, "Implementation of RGB and grayscale images in plant leaves disease detection-comparative study," *Indian Journal of Science and Technology*, vol. 9, (6), pp. 1-6, 2016.
- [16] Z. Xu, X. Baojie and W. Guoxin, "Canny edge detection based on open CV," in *2017 13th IEEE International Conference on Electronic Measurement & Instruments (ICEMI)*, 2017, .
- [17] R. Jain, R. Kasturi and B. G. Schunck, *Machine Vision*. 1995.
- [18] Z. Xu, X. Baojie and W. Guoxin, "Canny edge detection based on open CV," in *2017 13th IEEE International Conference on Electronic Measurement & Instruments (ICEMI)*, 2017, .
- [19] X. Mao *et al*, "Introduction to Opencv3 programming," *Publishing House of Electronics Industry: Beijing, China*, 2015.